



ELSEVIER

Journal of Alloys and Compounds 317–318 (2001) 266–273

Journal of
ALLOYS
AND COMPOUNDS

www.elsevier.com/locate/jallcom

Crystal structure, magnetic and electronic properties of $\text{Co}_x\text{Fe}_{1-x}\text{MnP}$ system

B. Średniawa^a, R. Zach^{a,*}, P. Fornal^a, R. Duraj^a, A. Bombik^b, J. Tobola^b, S. Kaprzyk^b, S. Niziol^b, D. Fruchart^c, M. Bacmann^c, R. Fruchart^c, J. Stanek^d

^aInstitute of Physics, Technical University of Cracow, Podchorążych 1, Cracow, Poland

^bFaculty of Physics and Nuclear Techniques, AGH, Al. Mickiewicza 30, Cracow, Poland

^cLaboratoire de Cristallographie, CNRS, BP 166X, Av. Martyrs, Grenoble, France

^dInstitute of Physics, Jagiellonian University, Reymonta 4, Cracow, Poland

Abstract

We present new results on the crystal structure, magnetic and electronic properties of the $\text{Co}_x\text{Fe}_{1-x}\text{MnP}$ series of compounds. X-ray diffraction experiments were performed for $x=0.525$, $x=0.65$ and $x=0.70$. A jump both of the lattice parameters and the unit cell volume was evidenced at the metamagnetic phase transition between antiferromagnetic and ferromagnetic states. Moreover the (P, T) magnetic phase diagrams for $x=0.45$, $x=0.50$ and $x=0.525$ were determined. Mössbauer spectroscopy experiments were performed for several x contents allowing to determine the hyperfine field, the isomer shift and the quadrupole splitting of the iron sites. Spin-polarised electronic structure calculations were performed using the Korringa–Kohn–Rostoker (KKR) method both for CoMnP and FeMnP , in the ferromagnetic state. The calculated local magnetic moments are $0.25 \mu_B$ (Co), $2.90 \mu_B$ (Mn) and $0.83 \mu_B$ (Fe), $2.89 \mu_B$ (Mn) in CoMnP and FeMnP , respectively. The electronic structure of the $\text{Co}_x\text{Fe}_{1-x}\text{MnP}$ solid solutions ($x=0.525$ and $x=0.70$) were calculated using the coherent potential approximation (CPA). The calculated values of the magnetic moments and hyperfine fields are compared with the experimental ones. © 2001 Elsevier Science B.V. All rights reserved.

Keywords: Magnetic phase transitions; Mössbauer spectroscopy; KKR–CPA calculations; High pressure; X-ray diffraction

1. Introduction

Crystal structure and magnetic properties of the $\text{Co}_x\text{Fe}_{1-x}\text{MnP}$ series of solid solutions appear strongly correlated in the vicinity of critical point in (x, T) phase diagram (Fig. 1) [1].

In this system of solid solutions in the whole composition range the compounds crystallise in the orthorhombic crystal structure of Co_2P -type ($Pnma$ space group). For $x < 0.5$ and $T \leq 250$ K this series of compounds exhibits exclusively antiferromagnetic properties, however for $x > 0.5$ both the antiferro–ferromagnetic and the ferro-paramagnetic phase transitions have been evidenced in (x, T) phase diagram [1]. FeMnP has an orthorhombic structure at room temperature but transforms into the hexagonal Fe_2P type crystal structure at 1473 K [2]. Neutron diffraction measurements carried out on the orthorhombic phase revealed a non-collinear antiferromagnetic structure with magnetic moments 0.5 and $2.6 \mu_B$ at 125 K for iron and

manganese atoms, respectively [3]. Mössbauer spectroscopy analyses [4] indicate that magnetic ordering takes place below 265 K. Below 170 K the ^{57}Fe spectra reveal a remarkable distribution of hyperfine fields. It is stressed that such a distribution may arise from the magnetic structure of a helical type, spin direction modulated.

CoMnP compound exhibits ferromagnetic properties with rather high Curie temperature (~ 600 K). At low temperatures a complex incommensurate magnetic structure was established [5].

Band structure calculations on CoMnP were carried out by the LMTO method [6]. The calculated magnetic moments of cobalt and manganese atoms are 0.06 and $3.13 \mu_B$, respectively. These values are in good agreement with the neutron diffraction and magnetisation measurements [3].

The aim of this work was to constitute experimental investigations and theoretical interpretations of magnetic properties for several contents of $\text{Co}_x\text{Fe}_{1-x}\text{MnP}$ series of compounds. Special attention was being paid for the crystal lattice parameters, the atomic position parameters, the isomer shifts and the hyperfine fields of some com-

*Corresponding author.

E-mail address: puzach@cyf-kr.edu.pl (R. Zach).

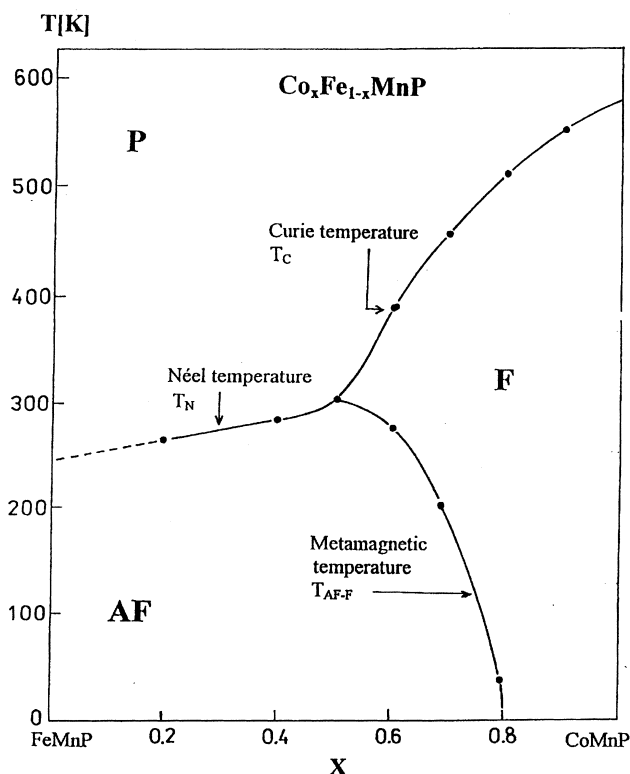


Fig. 1. (x, T) magnetic phase diagram for $\text{Co}_x \text{Fe}_{1-x} \text{MnP}$ series of compounds [1]. AF, F, P — denote antiferromagnetic, ferromagnetic and paramagnetic states, respectively.

pounds versus temperature and composition. Moreover, the influence of external pressure on magnetoelastic phase transitions observed in several contents was studied. On the basis of the experimentally detected crystal structure parameters electronic structure calculations were performed for selected compounds. Finally, the computed values of the magnetic moments and the hyperfine fields were compared with the experimental data.

In this work X-ray diffraction experiments ($x=0.525$, $x=0.65$ and $x=0.70$), Mössbauer spectroscopy analysis ($x=0.45$, $x=0.525$, $x=0.65$ and $x=0.70$) and a.c. susceptibility measurements under hydrostatic pressure ($x=0.45$, $x=0.50$ and $x=0.525$) were undertaken. Moreover, electronic structure calculations by the Korringa–Kohn–Rostoker method and combined with the coherent potential approximation (KKR–CPA) [7,8] were performed for the CoMnP and FeMnP compounds as well as for the $\text{Co}_x \text{Fe}_{1-x} \text{MnP}$ system ($x=0.525$ and $x=0.70$), respectively.

2. Experimental

Polycrystalline samples were synthesised starting from the appropriate proportions of 99.9% pure elements. Mixtures of fine powder were mixed, then progressively heated up to 850°C for 8 days in evacuated silica tubes. The final heat treatment performed by high frequency

heating allowed to melt the sample and then anneal by cooling down.

X-ray diffraction experiments for the samples with $x=0.525$, $x=0.65$, $x=0.70$ were performed on the Philips diffractometer (Bragg–Brentano geometry) in 80–400 K temperature range.

A.c. susceptibility measurements under pressure were carried out in the temperature range of 80–400 K on an apparatus based on the high pressure compressor (up to 1.5 GPa). Gaseous helium was used as a pressure transmitting medium. A manganin pick-up coil as a pressure sensor was used. The temperature was measured by means of copper-constantan thermocouple placed in direct contact with the sample. The signal produced in a system of three pick-up coils (series opposition) by an a.c. magnetic field (≈ 1 mT), was addressed to a lock-in nanovoltmeter. The Curie temperature was defined as the abscissae of the inflection point at the a.c. susceptibility vs. temperature curve, and the Néel point as the maximum in the a.c. susceptibility vs. temperature curves.

The Mössbauer spectra were recorded in transmission geometry using a ^{57}Co in Rh source of 40 mCi activity. Grounded samples, mixed with lucide powder, were prepared in a form of pellets of 18 mm in diameter. The low temperature measurements were carried out in a gas-flow nitrogen cryostat where the temperature was stabilised by a build-in oven within an accuracy of 1 K.

3. Results and discussion

3.1. Experimental study

X-ray diffraction measurements of $\text{Co}_x \text{Fe}_{1-x} \text{MnP}$ system ($x=0.525$, $x=0.65$, $x=0.70$) were carried out at different temperatures in order to characterise the magnetoelastic properties of the system. The Rietveld profile refinement method was used in order to determine the cell and the atomic position parameter as reported in Table 1. In all the refinements a Gaussian type profile of the Bragg peaks was used. Several patterns collected in the temperature range from 90 to 400 K were obtained, allowing to determine the thermal behaviour of the lattice parameters and volume as presented in Fig. 2. The values of lattice parameters at room temperature remains in good agreement with those previously determined [1]. A jump in the lattice parameters and in the unit cell volume, associated with the metamagnetic phase transition, was found in all the studied compounds. The values of the relative jump in the unit cell volume $\Delta V/V$ are of the order of 0.3–0.7%. Except for the temperatures about the phase transition the temperature dependence of the lattice parameters as well as of the unit cell volume was found to be approximately linear. In the case of the sample with $x=0.525$ the two changes in the temperature dependence of the lattice

Table 1

Lattice parameters and atomic position parameters of $\text{Co}_x\text{Fe}_{1-x}\text{MnP}$ refined at room temperature

	$x=0.525$	$x=0.65$	$x=0.70$
a [Å]	5.9472	5.9429	5.9421
b [Å]	3.5516	3.5317	3.5230
c [Å]	6.7452	6.7318	6.7326
V [Å ³]	142.472	141.289	140.939
$(x_{\text{Co}}, z_{\text{Co}})$	0.850(6), 0.065(8)	0.855(8), 0.063(9)	0.851(1), 0.062(4)
$(x_{\text{Fe}}, z_{\text{Fe}})$	0.850(6), 0.065(8)	0.855(8), 0.063(9)	0.854(1), 0.062(4)
$(x_{\text{Mn}}, z_{\text{Mn}})$	0.973(4), 0.672(2)	0.973(5), 0.067(1)	0.969(2), 0.670(1)
$(x_{\text{P}}, z_{\text{P}})$	0.232(6), 0.125(6)	0.228(3), 0.127(2)	0.230(5), 0.129(4)

parameters, should be associated with AF–F and F–P phase transitions, respectively.

Temperature dependence of a.c. susceptibility of $\text{Co}_x\text{Fe}_{1-x}\text{MnP}$ system ($x=0.45$, $x=0.50$, $x=0.525$) was studied under pressure up to 1.5 GPa (Fig. 3a). On the basis of these data the pressure dependence of the metamagnetic, the Curie and the Néel temperatures and the (P , T) magnetic diagrams were determined (Fig. 3b). In the case of $x=0.50$ and $x=0.525$ the Curie temperature increases vs. pressure ($dT_{\text{C}}/dP=4.0$ K/GPa for $x=0.50$

and $dT_{\text{C}}/dP=5.5$ K/GPa for $x=0.525$). For these samples the pressure dependence of the phase transition temperature between the AF–F states was also found and it decreases with increasing pressure ($dT_{\text{AF-F}}/dP=-6.2$ K/GPa for $x=0.5$ and $dT_{\text{AF-F}}/dP=-5.6$ K/GPa for $x=0.525$). For $x=0.45$ an antiferromagnetic–paramagnetic phase transition was established with the Néel temperature slightly increasing with pressure ($dT_{\text{N}}/dP=0.8$ K/GPa).

⁵⁷Fe Mössbauer spectroscopy experiments were carried out on the samples with $x=0.45$, $x=0.525$, $x=0.65$ and

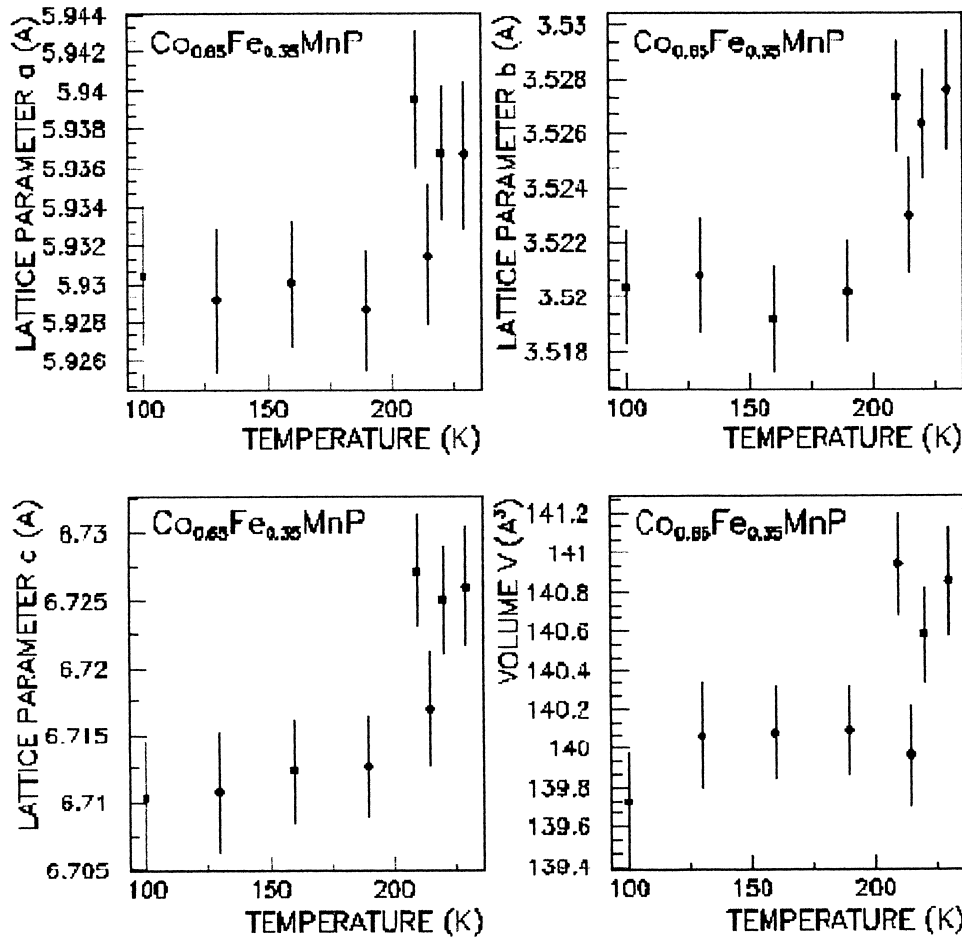
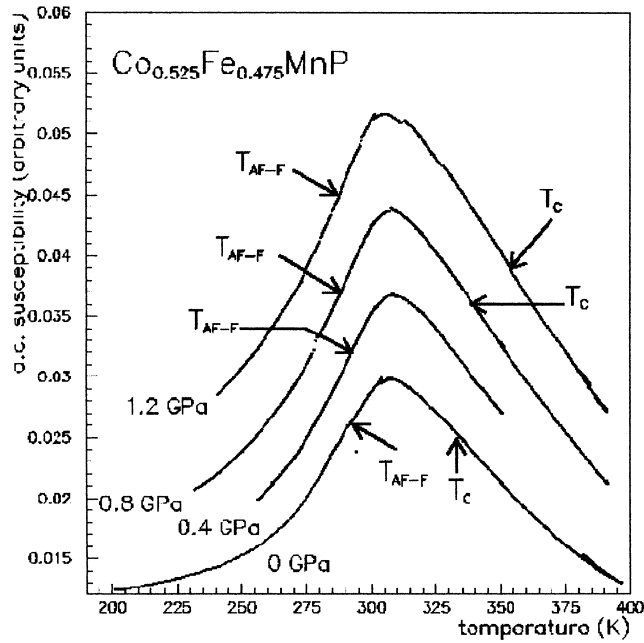
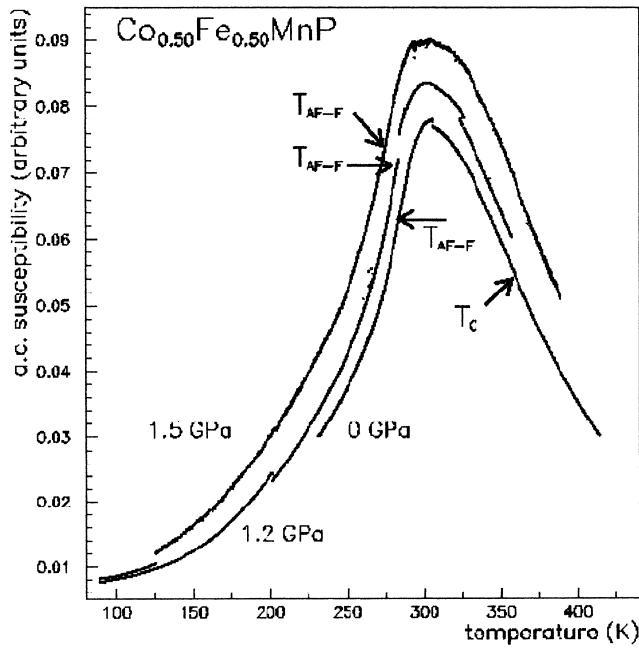
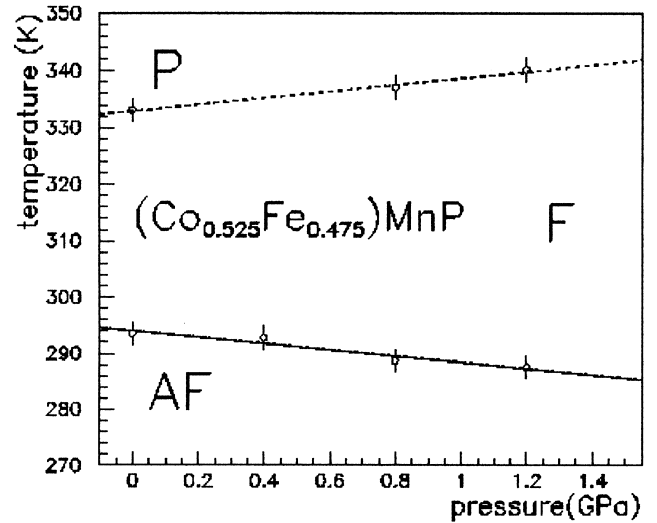
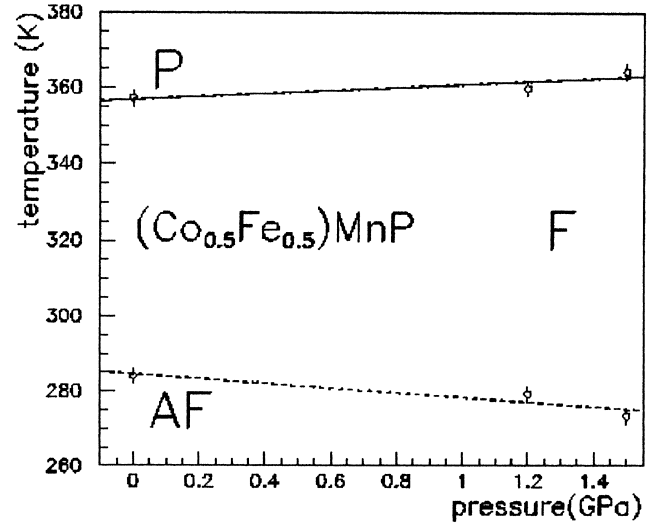
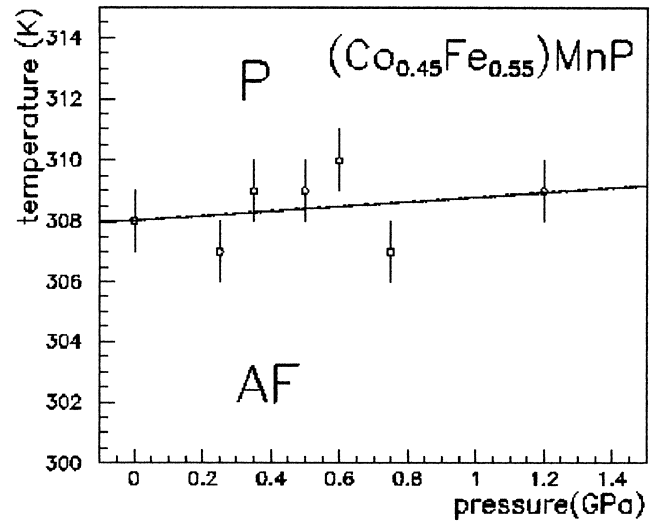


Fig. 2. Temperature dependence of the lattice parameters and the elementary unit cell volume for the $\text{Co}_{0.65}\text{Fe}_{0.35}\text{MnP}$ sample.



(a)



(b)

Fig. 3. (a) Temperature dependence of a.c. susceptibility runs for $x=0.5$ and $x=0.525$ for selected pressures; T_{AF-F} is the metamagnetic (antiferro-ferromagnetic) transition temperature, T_c is the Curie temperature. (b) (P, T) magnetic phase diagrams for $x=0.45$, $x=0.50$ and $x=0.525$. AF, F, P — denote antiferromagnetic, ferromagnetic and paramagnetic regions, respectively.

$x=0.70$ at liquid nitrogen temperature and at room temperature. The transmission Mössbauer spectra collected at RT and LN_2 are shown in Figs. 4 and 5, respectively. The spectra of all the samples show a clear magnetic splitting at LN_2 temperature while at RT the samples with $x=0.45$ and $x=0.525$ are paramagnetic. The sample with $x=0.70$ is completely magnetic and in the case of $x=0.65$ paramagnetic and magnetic fractions coexist. The Mössbauer spectra were fitted assuming the Gaussian type of hyperfine fields H_{eff} distribution. The distributions obtained for the samples measured at LN_2 temperature are shown in Fig. 5. The value of isomer shift (δ) and quadrupole shift (Δ) of a magnetic pattern [9] were not correlated with magnetic field so the spectra were fitted with one value of δ and Δ . The obtained values of the hyperfine parameters are collected in Table 2.

The unique values of δ and Δ suggests that iron is located in one crystallographic site which is consistent with X-ray analysis. The above distribution of H_{eff} , is not

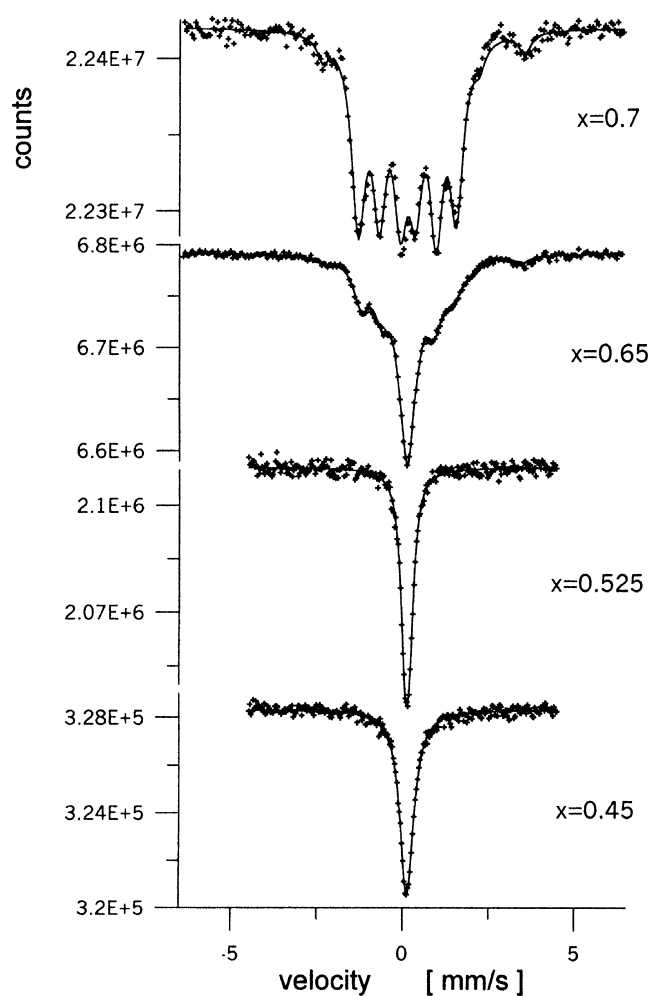


Fig. 4. ^{57}Fe Mössbauer spectra of $\text{Co}_x\text{Fe}_{1-x}\text{MnP}$ measured at room temperature for selected iron contents. The solid lines are the least-square fits with assumption of the Gaussian type distribution of magnetic field.

surprising, it is commonly observed for specimens with statistical distributions as here with cobalt and iron atoms.

For samples with higher cobalt content i.e. $x=0.7$ and $x=0.65$ an additional small component was observed in the Mössbauer spectra. This component characterised by significantly higher δ and stronger H_{eff} is assigned to a ferromagnetic fraction (Table 2).

Magnetic properties of the samples are strongly composition dependent. The temperature of magnetic ordering increases with an increase in the cobalt content, cf. Fig. 4.

The reduction of internal magnetic field is related to the local states of iron. For certain iron contents due to statistical distribution of cations the exchange interactions averages to very low absolute value thus yielding fast fluctuations of the spatial orientation of iron magnetic moments.

In spite of the crystalline homogeneity and well established long range magnetic ordering some compounds at certain temperatures can be qualified as magnetically heterogeneous because of local character of the Mössbauer spectroscopy.

3.2. Theoretical study

The KKR-CPA electronic structure [7,8] calculations were performed on $\text{Co}_x\text{Fe}_{1-x}\text{MnP}$ with $x=0.525$, $x=0.65$, $x=0.70$ using the crystal structure parameters as derived from our X-ray measurements (Table 1). Additionally, the electronic band structure of the parent compounds were calculated by the KKR method, along the same line as in [8]. In CoMnP the calculated total magnetic moment of $3.03 \mu_B$ remains in excellent agreement with the experimental data and with the previous LMTO calculations [6]. However, the local magnetic moments on Co ($0.25 \mu_B$) and Mn ($2.91 \mu_B$) are slightly larger than the values derived from neutron diffraction measurements [3]. Conversely, the sum of the magnetic moments in FeMnP ($3.62 \mu_B$) results larger than in CoMnP , since a contribution of the tetrahedral site $\mu_{\text{Fe}}=0.83 \mu_B$ is larger. However the magnetic moments computed here correspond well to the experimental values [3]. Moreover, it is also worth noting that the theoretical magnetic moment on the iron site in FeMnP is smaller than the value found in the hexagonal phase of FeMn(P-As) [10–13].

Looking at the total density of states in both compounds (Fig. 6) one can notice that $N(E_F)$ in FeMnP (141 states/Ry/cell) is markedly enhanced in comparison with $N(E_F)$ in CoMnP (43.8 states/Ry/cell) which may tentatively explain the magnetic instability in FeMnP , turning the system to the antiferromagnetic state. Moreover the DOS of Fe impurity in the $\text{Co}_x\text{Fe}_{1-x}\text{MnP}$ ($x=1.0$) already displays the spin-polarisation rising its magnetic moment to $0.56 \mu_B$. This may explain a slight increase in the average magnetic moment of the tetrahedral position while passing from CoMnP to FeMnP . On the other hand, the magnetic moment of Mn does not vary significantly with

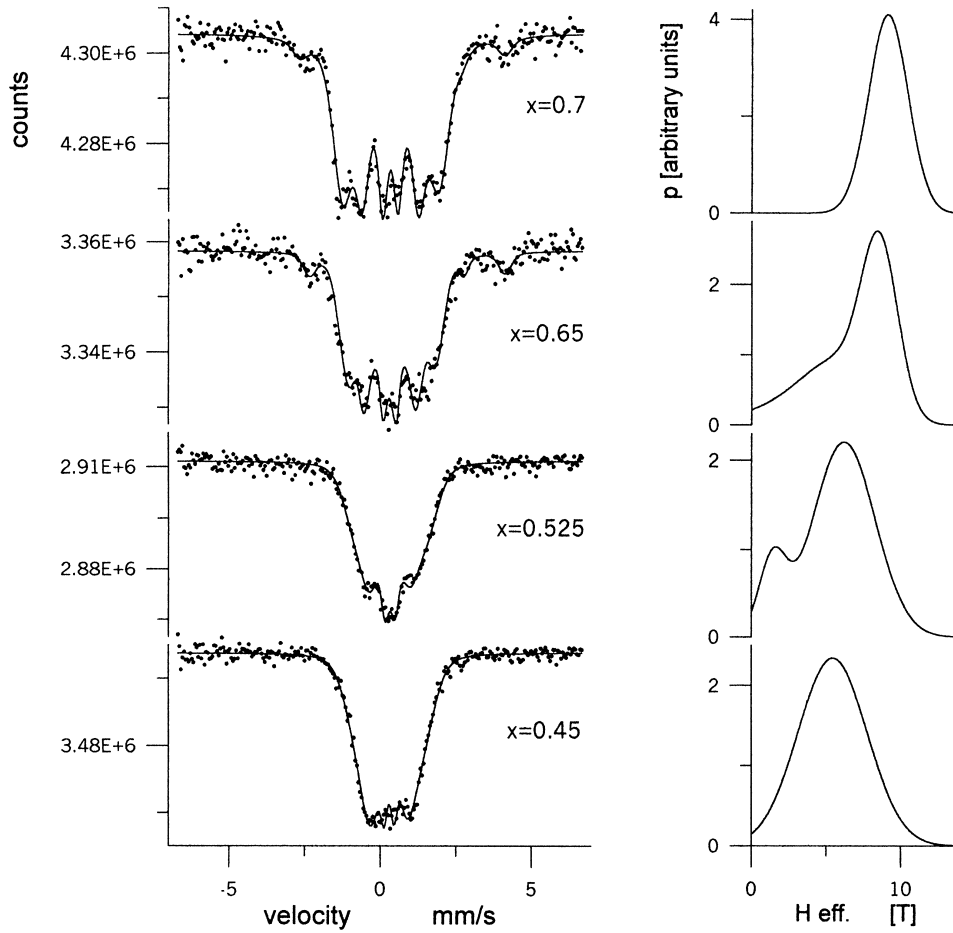


Fig. 5. ⁵⁷Fe Mössbauer spectra of Co_xFe_{1-x}MnP measured at liquid nitrogen temperature (left) and corresponding distributions of effective magnetic field H_{eff} (right) in the antiferromagnetic state. The contribution of small ferromagnetic fraction is not shown in the H_{eff} distributions.

Table 2
Mössbauer parameters of Co_xFe_{1-x}MnP measured at liquid nitrogen (LN₂) and room temperature (RT)^a

x	LN ₂					RT				
	δ (mm/s)	Δ (mm/s)	H_{eff}		F (%)	δ (mm/s)	Δ (mm/s)	H_{eff}		F (%)
			Centre (T)	Sigma (T)				Centre (T)	Sigma (T)	
0.7	0.33	0.007	10.0	1.3	74	0.29	0.01	8.7	0	89
			3.7	3.8	19	0.26	0	0	0	3
	0.61	0	21.1	0.87	7	0.69	0.05	18.3	0	8
0.65			9.3	0.63	47	0.30	0.01	8.2	0	69
	0.33	0.2	6.3	0.43	14	0.29	0	0	0	26
			3.0	3.5	28					
0.525			20.1	1.4	10	0.56	0.2	17.7	0	5
			9.0	0.61	25					
	0.33	0.17	6.2	0.42	56	0.29	0.6	0	0	100
0.45			1.7	0.11	19					
	0.32	0.02	5.9	2.5	100	0.29	0.6	0	0	100

^a δ-isomer shift, Δ-quadrupole shift of magnetic pattern in case of magnetically ordered samples or quadrupole splitting in the case of paramagnetic state ($H_{\text{eff}}=0$); H_{eff} — effective magnetic field; Centre and Sigma are parameters of Gaussians distributions of H_{eff} ; F — fraction of each component.

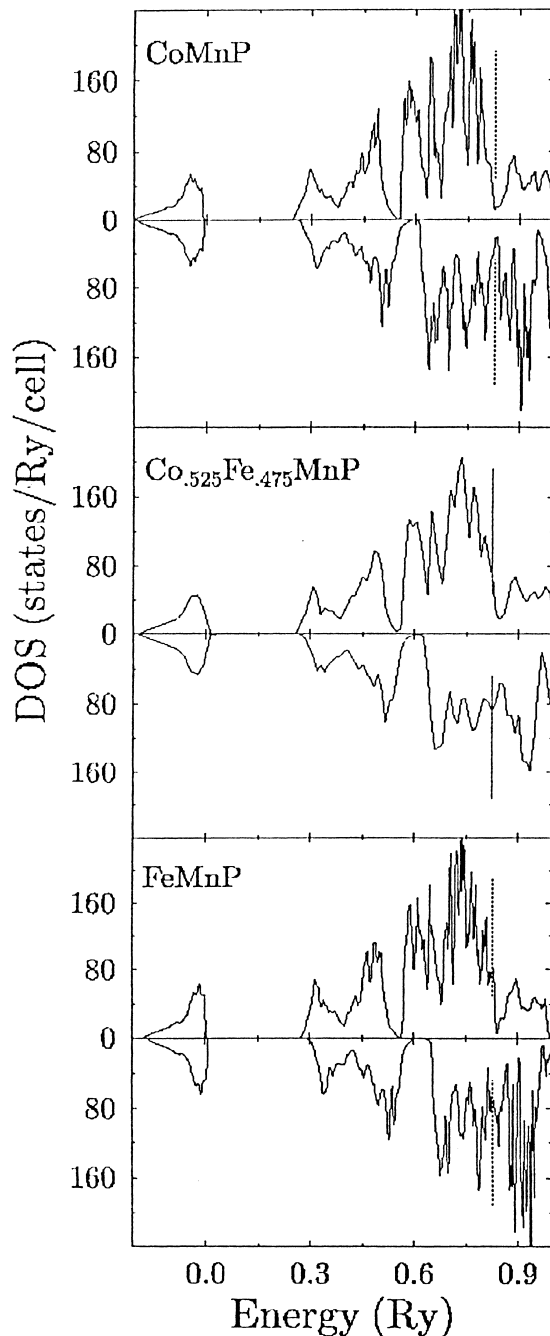


Fig. 6. Total electronic density of states in CoMnP, $\text{Co}_{0.525}\text{Fe}_{0.475}\text{MnP}$ and FeMnP calculated by KKR–CPA method. Vertical dotted lines indicate the Fermi energy.

composition. From the KKR–CPA DOS we conclude, that total $N(E_F)$ successively increases while replacing Co with Fe in (Co–Fe)MnP, mostly due to the Fermi level crossing spin-minority DOS peak attributed to Fe and Co sites. In comparison to CoMnP, $N(E_F)$ has larger values in $\text{Co}_{0.7}\text{Fe}_{0.3}\text{MnP}$ (157 st./Ry/cell) and $\text{Co}_{0.525}\text{Fe}_{0.475}\text{MnP}$ (162 st./Ry/cell). The calculated local magnetic moments for selected compositions are presented in Table 3.

Furthermore, the values of the hyperfine fields were

Table 3

Atomic moments (in μ_B) in the orthorhombic $\text{Co}_x\text{Fe}_{1-x}\text{MnP}$ from the KKR–CPA calculations

	Total/f.u.	Co	Fe	Mn	P
$\text{Co}_{1.0}\text{Fe}_{0.0}\text{MnP}$	3.03	0.25	0.56	2.91	–0.07
$\text{Co}_{0.7}\text{Fe}_{0.3}\text{MnP}$	3.17	0.26	0.60	2.93	–0.07
$\text{Co}_{0.525}\text{Fe}_{0.475}\text{MnP}$	3.33	0.28	0.70	2.97	–0.07
FeMnP	3.62	–	0.83	2.89	–0.06

derived from the spin-density at the iron nucleus (within the Fermi contact formula). It is found to be 11.0 and 12.1 T in the case of $x=0.70$ and $x=0.475$ contents, respectively. In the approach of purely ferromagnetic state of $\text{Co}_x\text{Fe}_{1-x}\text{MnP}$, theoretical results remain in a satisfactory agreement with our Mössbauer data. However slightly smaller values of the hyperfine field can be expected from the KKR–CPA calculations using the LSD approximation. This effect may originate either from the spherical approximation applied in our method or from complex magnetic structure occurring in the studied samples. This should be addressed to forthcoming investigations.

4. Conclusions

To conclude this work some general features of $\text{Co}_x\text{Fe}_{1-x}\text{MnP}$ series of compounds could be mentioned:

1. The lattice parameters as well as atomic position parameters for the $\text{Co}_x\text{Fe}_{1-x}\text{MnP}$ solid solutions ($x=0.525$, $x=0.65$ and $x=0.70$) were determined.
2. For all the studied contents (i.e. $x=0.45$, $x=0.50$, $x=0.525$) the (P , T) magnetic phase diagrams were established. The Curie temperature T_C and the Néel temperature T_N linearly increases with pressure. However, the metamagnetic (AF–F) phase transition temperature shows slight linear decrease vs. applied external pressure.
3. The AF–F metamagnetic phase transition at T_i as well as the F–P transition at T_C reveal the magnetoelastic properties. The abrupt changes in the unit cell volume (about 0.3–0.7%) were evidenced at both phase transitions.
4. The isomer shift, the quadrupole shift, the quadrupole splitting and the hyperfine field were determined for selected cobalt contents; it may be concluded that in spite of the homogeneity of the samples and well established long range magnetic ordering, some compounds can be qualified as locally magnetically heterogeneous.
5. The electronic structure calculations were performed for the $\text{Co}_x\text{Fe}_{1-x}\text{MnP}$ alloys. The theoretical values of magnetic moments and hyperfine fields remain in good agreement with the experimental results. Moreover the evolution of the KKR–CPA density of states in the vicinity of the Fermi level, when passing from CoMnP

to FeMnP, may tentatively explain experimentally detected AF–F magnetic transition.

References

- [1] A. Roger, Thesis, Paris, 1970.
- [2] B. Chenevier, J.L. Soubeyroux, M. Bacmann, D. Fruchart, R. Fruchart, *Solid State Commun.* 64 (1987) 57.
- [3] T. Suzuki, Y. Yamaguchi, H. Yamamoto, H. Watanabe, *J. Phys. Soc. Jpn.* 34 (1973) 911.
- [4] J. Sjöström, L. Häggström, T. Sundqvist, *Phil. Mag.* B57 (1988) 737.
- [5] P. Radhakrishna, H. Fujii, S. Doniach, W. Reichardt, P. Charpin, *J. Magn. Magn. Mater.* 70 (1987) 229.
- [6] S. Fujii, S. Ishida, S. Asano, *J. Phys. F: Metal Phys.* 18 (1988) 971.
- [7] S. Kaprzyk, *Acta Phys. Pol. A* 91 (1997) 135.
- [8] A. Bansil, S. Kaprzyk, P.E. Mijnarends, J. Tobola, *Phys. Rev. B* 60 (1999) 13396.
- [9] P. Gütlich, in: U. Gonser (Ed.), *Mössbauer Spectroscopy — Topics in Applied Physics*, Vol. 5, Springer-Verlag, Berlin, Heidelberg, New York, 1975, p. 67.
- [10] J. Tobola, M. Bacmann, D. Fruchart, S. Kaprzyk, A. Koumina, S. Niziol, J.L. Soubeyroux, P. Wolfers, R. Zach, *J. Magn. Magn. Mater.* 157–158 (1996) 708.
- [11] R. Zach, M. Bacmann, D. Fruchart, P. Wolfers, R. Fruchart, M. Guillot, S. Kaprzyk, S. Niziol, J. Tobola, *J. Alloys Comp.* 262–263 (1997) 508.
- [12] R. Zach, M. Guillot, J. Tobola, *J. Appl. Phys.* 83 (1998) 7237.
- [13] R. Zach, *Zesz. Nauk. Politechnika Krakowska*, Vol. 21, Nr. 2 (1997).